J Electroceram (2012) 29:42–55
DOI 10.1007/s10832-012-9736-1

Experimental model identification and vibration control of a smart cantilever beam using piezoelectric actuators and sensors

Tamara Nestorović · Navid Durrani · Miroslav Trajkov

Received: 25 September 2011 / Accepted: 30 April 2012 / Published online: 17 May 2012

Abstract Mechanical lightweight structures often tend to unwanted vibrations due to disturbances. Passive methods for increasing the structural damping are often inadequate for the vibration suppression, since they include additional mass in the form of damping materials, additional stiffening designs or mass damper. In this paper the concept of an active vibration control for piezoelectric light weight structures is introduced and presented through several subsequent steps: model identification, controller design, simulation, experimental verification and implementation on a particular object—piezoelectric smart cantilever beam. Special attention is paid to experimental testing and verification of the results obtained through simulations. The efficiency of the modeling procedure through the subspace-based system identification along with the efficiency of the designed optimal controller are proven based on the experimental verification, which results in vibration suppression to a very high extent not only in comparison with the uncontrolled case, but also in comparison with previously achieved results. The experimental work demonstrates a very good agreement between simulations and experimental results.

Keywords Active vibration control · Piezoelectric cantilever beam · Subspace identification · Optimal controller · Kalman estimator · Experimental verification

T. Nestorović (✉) · N. Durrani · M. Trajkov
Mechanics of Adaptive Systems, Ruhr-Universität Bochum,
Universitaetsstr. 150, Building IA 01/128,
D-44801 Bochum, Germany
e-mail: tamara.nestorovic@rub.de

1 Introduction and motivation

High efficiency, functionality, quality and assuring a high profitability are the main requirements for products in today's world. In mechanical and civil engineering, these requirements are manifested in the application of thin and lightweight structures. Mechanical lightweight structures often tend to unwanted vibration, which may result in disturbing sound radiation or even in damage of components, [1]. Passive methods for increasing the structural damping are often inadequate, because they always include the use of additional mass in the form of damping materials, additional stiffening designs or mass damper.

The concept of active vibration control has become a useful approach in the recent years, due to improvement of the vibration susceptibility of lightweight structures with the least possible increase in mass. For the active vibration control, supporting mechanical structure is supplied with sensors and actuators operated by a controller. High integration of the structural system with active materials (actuators/sensors) and control is regarded as a smart structure due to its ability to adapt to environmental changes. The technology of smart materials and structures, especially piezoelectric smart structures, has become mature over the last decade. One promising application of piezoelectric smart structures is the control and suppression of unwanted structural vibrations [2].

2 State of the art

Smart structures have been intensively investigated in the past years. In numerous studies the smart structure community has developed a large variety of sophisticated analysis approaches, control methods and optimization procedures.

A review of the state of the art of smart structures is given by Chopra [3] and some other examples of analytical and experimental studies concerning the actuation and vibration control of smart piezoelectric structures can be found in [4–10].

Investigation of the vibration suppression of flexible structures with integrated piezoelectric active materials has been subject of a very high scientific and practical interest over the past years. One benchmark test example, vibration suppression of a piezoelectric cantilever beam, represents in the scientific community a research object of a special interest for many researches within the area, since it offers the possibility to investigate, test and compare different approaches, techniques and results.

In this paper an overall approach to active control of piezoelectric structures is presented and implemented for the vibration suppression of a smart cantilever beam subjected to external disturbances. The procedure involves several subsequent steps: model identification, controller design, simulation, experimental verification and implementation.

Different approaches to modeling and vibration suppression of a piezoelectric cantilever beam have been investigated and reported in the literature. In [11] for example the effect of different types of controllers to vibration reduction of the beam have been studied. In [12] the feedback control with a time delay was used in the investigation of vibration control for the primary resonance of a cantilever beam. The analytical results are compared with numerical simulations.

With design and implementation of the spatial H_∞ controller has been dealt with in [13]. Here the standard modeling approach by modal truncation was applied and the H_∞ controller was designed to suppress the first two flexural vibrations of the beam.

Modeling and controller design technique used in the present paper was successfully applied for the vibration suppression of higher bending modes then investigated in [12, 13]. Proposed controller in combination with augmented plant dynamics [6–8] can be successfully used in the presence of combined disturbances and for the vibration suppression of even higher modes.

In [14] active vibration control of a flexible cantilever beam was studied using the Filtered-X LMS algorithm, applied to design a control law for a piezoelectric actuator. In comparison with this algorithm, the technique with the optimal LQ controller and Kalman estimator proposed and applied in the present paper results in considerably faster controlled response in the time domain, and in higher vibration magnitude suppression in the frequency domain.

Paper by Tjahyady et al. [15] also deals with the vibration control of a flexible cantilever beam. The control technique applied here is adaptive resonant control. For the controller design purposes, the model of the beam, i.e. its first three natural frequencies were estimated using the RLS algorithm. In the present paper the model development procedure is based on the subspace based identification algorithm (n4sid). The proposed identification procedure is of special interest if a state space model of the structure is required for the subsequent design and analysis phases. State space models are especially convenient for the multiple-input multiple output (MIMO) control design problems. In [14] a single-input single-output model was considered.

Further literature records also document implementation of active vibration control of piezoelectric cantilever beams. The controller applied in [16] for the active vibration control of a flexible steel cantilever beam with piezoelectric actuators is PID compensator with optimized parameters. In [17] the problem of a semi-analytical analyzing of the dynamic steady-state response of locally nonlinear beams under piezoelectric actuation has been treated. Special attention has been paid to elastic beam structures with time-variant imposed piezoelectric curvature. Other examples of active piezoelectric cantilever beams and their vibration compensation are presented in [18–22]. Recently published papers further document strong interest of the scientific community in the field of active vibration suppression of piezoelectric structures. In [20] the vibration suppression of a smart flexible beam has been performed by active fuzzy logic based control, using piezoelectric sensor and actuator. Similarly, a neuro-fuzzy control supplemented by proportional-derivative PD control based on genetic algorithm is proposed in [23] for vibration suppression of a smart piezoelectric rotating truss structure. The contribution confirms that elementary smart structures, like beam or truss structures, can successfully be implemented as elements of more complex smart systems with active piezoelectric based control. Another work, [24] documents again the implementation of PD controller for vibration suppression of a piezoelectric sandwich beam. In this case the modeling of the beam dynamics was performed by highly nonlinear ordinary differential equation. In order to model piezoelectric properties of smart structures, in [25] the authors have considered the implementation of a user-defined piezoelectric finite shell element. The element efficiency was tested through several examples of a bimorph piezoelectric beam. Modeling approach applied in [26] is an approximate formulation for the coupled electromechanical problem of forced vibration of a simply supported inelastic sandwich beam with piezoelectric layers. Single-frequency forced vibrations are damped in this case by harmonic voltages applied to the external piezoelectric active layers. Some of other recent studies on active piezoelectric beams are presented in [27–29]. Mentioned references are only some of the numerous investigations of the controlled piezoelectric cantilever beam behavior, with the aim of vibration suppression and they all treat the same or similar objects in a different manner. All these examples document a tremendous interest of the scientific community in the problem of the

smart beam control and vibration suppression and therefore confirm the importance of this filed, which is still not entirely exploited.

In this paper, the authors propose the subspace identification procedure for the state space model development of the aluminium cantilever beam with four piezoelectric patches. In this way the MIMO model is identified, which can be successfully implemented in the controller design procedure. For the controller design an optimal LQ technique is proposed in combination with the Kalman filter based estimation of the plant model state variables. According to the authors' best knowledge, this methodology has not been previously implemented for the vibration suppression of cantilever piezoelectric beams. Special attention is paid to experimental testing and verification of the results obtained through simulations. The efficiency of the modeling procedure through the system identification along with the efficiency of the designed controller are proven based on the experimental verification, which results in vibration suppression to a very high extent not only in comparison with the uncontrolled case, but also in comparison with previously achieved results. The experimental work demonstrates a very good agreement between simulations and experimental results.

In the first part of the paper description of the active structure (cantilever beam with piezoelectric patches) and its modeling are presented. Modeling procedure involves experimental subspace-based system identification. Second part is devoted to an optimal controller design, which incorporates Kalman filter for estimation of the unmeasurable state variables. Simulation of the control action is performed for several excitation cases. Finally, the controller was verified experimentally using a hardware-in-the-loop testing system. Experimental results prove the efficiency of the controller and the reliability of the identified model, which was used as the basis for the controller design.

3 Mechanical structure

Flexible smart structure shown in Fig. 1 is used as an experimental object to test the effectiveness of the proposed vibration suppression method. The smart structure consists of a cantilever aluminum beam (Young's modulus 70 GPa and density 2.7 g/cm³) and four piezoelectric patches (DuraActTM P-876.A15), which are attached to the beam, two on each side of the beam. These four patches are used as actuators to enable active vibration control of the beam.

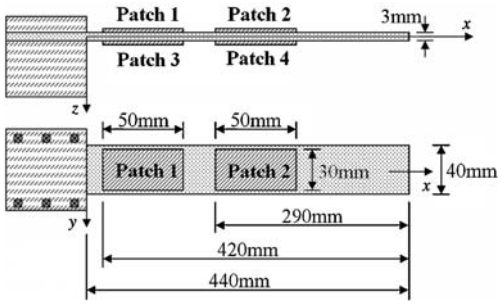

Fig. 1 Geometry and layout of the smart structure

A scanning digital laser Doppler vibrometer (VH-1000-D), which acts as a sensor, is used to measure the velocity of the bending vibration at a certain point, near the free end of the beam. The sensor provides the feedback signal in the active control algorithm as presented in Fig. 2.

In this experiment the plant has four voltage inputs, one input for each piezoelectric actuator, and one output, which is recorded from the sensor. For implementing the controller in real time, a dSPACE digital data acquisition and real-time control system is used. The dSPACE uses a DS1005 digital signal process board for real-time control implementations. The dSPACE system is connected both to an analog-to-digital converter ADC Board DS2004 and to a digital-to-analog converter DAC Board DS2102, in order to process the continuous-time sensor signal and for generating a continuous-time series of control signal, respectively. The range of the DAC board is ±10 V. Since for the actuation of the piezoelectric patches much higher voltages are required, the control signal is fed out of the DAC board through the piezo-amplifier to the piezoelectric actuators. The control law, for the active suppression of the bending vibration, is designed on MATLAB platform and then downloaded to the dSPACE digital data acquisition and real-time control system to implement the proposed control algorithm.

An experimental modal analysis was performed in order to determine the eigenmodes of interest for the controller design. Longitudinal and torsional modes, which are not relevant for the bending vibration suppression, were not considered for the controller design. Bending mode shapes obtained through the experimental modal analysis are represented in Fig. 3. The experimental modal analysis has also shown that the dominant mode of the flexible beam is its first mode and is the major concern for vibration suppression.

4 System modeling

Controller design for smart structures relies on accurate modeling of the system dynamics. Models of smart structures can be obtained either by a numerical modeling based on finite element method (FEM) [30] or by an experimental model identification approach, the so-called subspace-based system identification [31]. The goal of the identification procedure in general is to find a model which can with sufficient accuracy predict the behavior of a system under consideration based on the measured input and output data. In case of the subspace-based identification the output of the identification procedure is

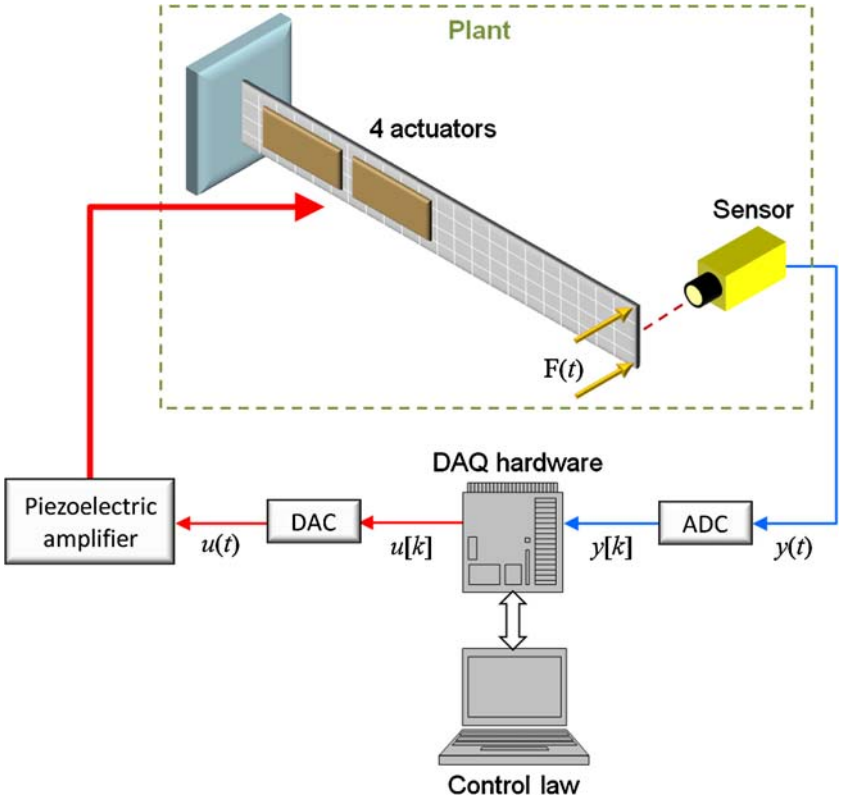

Fig. 2 Sketch of the experimental set-up

a state space model. The subspace-based identification is as an alternative to numerical modeling using the FEM approach, since in case of availability of the real structure it enables a successful modeling of multiple-input multiple-output (MIMO) systems based on the measurement of the input and output signals.

Furthermore for MIMO systems the state space representation is the only model that is convenient for the work in the computer aided control system design. Most optimal controllers can be effectively computed in terms of the state space model. Practical aspects of implementing the subspace identification methods for industrial applications are another reason for the consideration of this approach. Many industrial processes and structures can be accurately described by discrete-time linear state space models. Therefore in this paper the subspace identification is used to obtain experimentally a model of the piezoelectric smart structure in the state-space form.

4.1 Subspace-based state-space system identification

The state space representation of an *n*th-order system with *m* inputs and *l* outputs which is to be identified from the input–

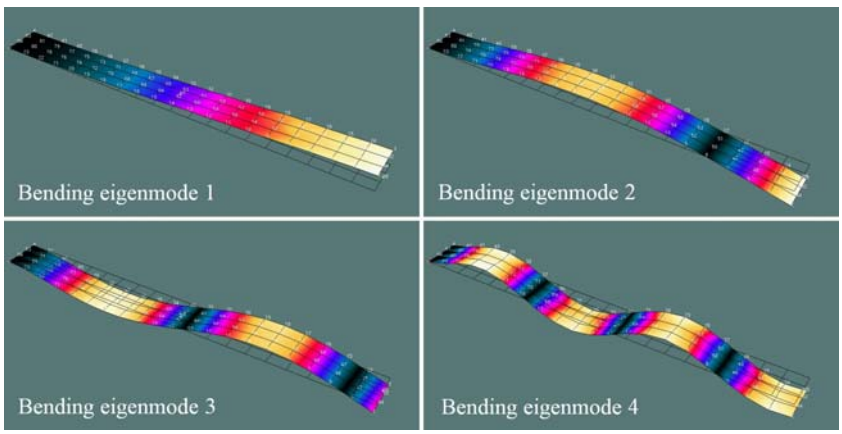

Fig. 3 Experimentally determined bending eingemodes of interest

output measurement data can be expressed in its general deterministic-stochastic form [32]:

$$\begin{aligned}\mathbf{x}[k+1] &= \mathbf{\Phi}\mathbf{x}[k] + \mathbf{\Gamma}\mathbf{u}[k] + \boldsymbol{w}[k] \\ \mathbf{y}[k] &= \mathbf{C}\mathbf{x}[k] + \mathbf{D}\mathbf{u}[k] + \boldsymbol{v}[k]\end{aligned} \tag{1}$$

Since the subspace identification is based on sampled input/output measurement sequences $\mathbf{u}[k]$ and $\mathbf{y}[k]$, the method applies to a discrete-time form of the resulting state-space model, with discrete-time state and control matrices $\mathbf{\Phi}$ and $\mathbf{\Gamma}$, respectively. The process noise and the measurement noise vector sequences $\boldsymbol{w}[k]$ and $\boldsymbol{v}[k]$ are white noise with zero mean and with covariance matrix:

$$E\left\{\begin{bmatrix}\boldsymbol{w}[i]\\ \boldsymbol{v}[j]\end{bmatrix}\begin{bmatrix}\boldsymbol{w}[i]^{\mathrm{T}} & \boldsymbol{v}[j]^{\mathrm{T}}\end{bmatrix}\right\} = \begin{bmatrix}\mathbf{Q} & \mathbf{S}\\ \mathbf{S}^{\mathrm{T}} & \mathbf{R}\end{bmatrix}, \tag{2}$$

The task of the subspace identification is to express the input-state-output relationships in the state space form (1) and to determine the order n of the unknown system and the system matrices $\mathbf{\Phi} \in R^{n\times n}$, $\mathbf{\Gamma} \in R^{n\times m}$, $\mathbf{C} \in R^{l\times n}$, $\mathbf{D} \in R^{l\times m}$ as well as the covariance matrices $\mathbf{Q} \in R^{n\times n}$, $\mathbf{S} \in R^{n\times l}$, $\mathbf{R} \in R^{l\times l}$ of the noise sequences $\boldsymbol{w}$[k] and $\boldsymbol{v}$[k]. In the subsequent derivations, only the pure deterministic case will be considered as described in [33].

Measured input and output data are arranged into block Hankel matrices [31] defined in the following way:

$$\mathbf{U} = U_{0|2i-1} = \left[\begin{array}{ccccc}\mathbf{u}_0 & \mathbf{u}_1 & \mathbf{u}_2 & \cdots & \mathbf{u}_{j-1}\\ \mathbf{u}_1 & \mathbf{u}_2 & \mathbf{u}_3 & \cdots & \mathbf{u}_j\\ \vdots & \vdots & \vdots & \ddots & \vdots\\ \mathbf{u}_{i-1} & \mathbf{u}_i & \mathbf{u}_{i+1} & \cdots & \mathbf{u}_{i+j-2}\\ \hline \mathbf{u}_i & \mathbf{u}_{i+1} & \mathbf{u}_{i+2} & \cdots & \mathbf{u}_{i+j-1}\\ \mathbf{u}_{i+1} & \mathbf{u}_{i+2} & \mathbf{u}_{i+3} & \cdots & \mathbf{u}_{i+j}\\ \vdots & \vdots & \vdots & \ddots & \vdots\\ \mathbf{u}_{2i-1} & \mathbf{u}_{2i} & \mathbf{u}_{2i+1} & \cdots & \mathbf{u}_{2i+j-2}\end{array}\right] \tag{3}$$

The output block Hankel matrix $\mathbf{Y}$ is defined in a similar way. The purpose of writing the matrix in this manner is to build the relations between the input, output and state sequences in a matrix form. Using the matrix notation, the system equation can be written as:

$$\mathbf{Y}[k] = \mathbf{G}\mathbf{x}[k] + \mathbf{H}\mathbf{U}[k] \tag{4}$$

The matrix $\mathbf{G}$ is the extended observability matrix built as

$$\mathbf{G} = \begin{bmatrix}\mathbf{C}\\ \mathbf{C\Phi}\\ \mathbf{C\Phi}^2\\ \vdots\\ \mathbf{C\Phi}^{i-1}\end{bmatrix} \in R^{li\times n} \tag{5}$$

and $\mathbf{H}$ is the lower block triangular Toeplitz matrix of impulse responses from $\mathbf{u}$ to $\mathbf{y}$ given by

$$\mathbf{H} = \begin{bmatrix}\mathbf{D} & 0 & 0 & \cdots & 0\\ \mathbf{C\Gamma} & \mathbf{D} & 0 & \cdots & 0\\ \mathbf{C\Phi\Gamma} & \mathbf{C\Gamma} & \mathbf{D} & \cdots & 0\\ \vdots & \vdots & \vdots & \ddots & \vdots\\ \mathbf{C\Phi}^{i-2}\mathbf{\Gamma} & \mathbf{C\Phi}^{i-3}\mathbf{\Gamma} & \mathbf{C\Phi}^{i-4}\mathbf{\Gamma} & \cdots & \mathbf{D}\end{bmatrix} \in R^{li\times n} \tag{6}$$

For a deterministic case the problem is simplified to determining $\mathbf{G}$ and $\mathbf{H}$ by computing the singular value decomposition (SVD) of $\mathbf{U}$ in the first step

$$\mathbf{U} = \mathbf{PSQ}^{\mathrm{T}} = [\,\mathbf{P}_{u1} \quad \mathbf{P}_{u2}\,][\,\Sigma_u \quad 0\,]\begin{bmatrix}\mathbf{Q}_{u1}^{\mathrm{T}}\\ \mathbf{Q}_{u2}^{\mathrm{T}}\end{bmatrix} \tag{7}$$

If matrix $\mathbf{U}$ has dimension $m \times n$ and rank r, then the partition in (7) is performed as follows:

$$\mathbf{P} = [\,\mathbf{p}_1 \quad \cdots \quad \mathbf{p}_r \,|\, \mathbf{p}_{r+1} \quad \cdots \quad \mathbf{p}_m\,] = [\,\mathbf{P}_{u1} \quad \mathbf{P}_{u2}\,] \tag{8}$$

$$\mathbf{Q} = [\,\mathbf{q}_1 \quad \cdots \quad \mathbf{q}_r \,|\, \mathbf{q}_{r+1} \quad \cdots \quad \mathbf{q}_m\,] = [\,\mathbf{Q}_{u1} \quad \mathbf{Q}_{u2}\,] \tag{9}$$

where $\mathbf{p}_i$ are the left singular vectors of $\mathbf{U}$. It can be shown that they are eigenvectors of UU^{T}. Vectors $\mathbf{q}_i$ are the right singular vectors of $\mathbf{U}$. It can be shown that they are eigenvectors of U^{T}UMultiplying (4) by $\mathrm{Q_{u2}}$ matrix $\mathbf{G}$ can be determined from a SVD of $\mathrm{YQ_{u2}}$ Then matrix $\mathbf{C}$ is obtained as the first row of the observability matrix $\mathbf{G}$, and matrix $\mathbf{\Phi}$ is calculated from: $\underline{\mathbf{G}} = \overline{\mathbf{G}}\mathbf{\Phi}$ applying pseudo inverse, where $\overline{\mathbf{G}}$ is obtained by dropping the last row of $\mathbf{G}$. Matrix $\underline{\mathbf{G}}$ represents the matrix obtained by dropping the first row of $\mathbf{G}$. For the calculation of the $\mathbf{\Gamma}$ and $\mathbf{D}$ matrices, (4) is multiplied by the pseudo inverse of $\mathbf{U}$ on the right and by $\mathbf{P}_{u2}^{\mathrm{T}}$ from (7) on the left. Thus the equation is reduced to

$$\mathbf{P}_{u2}^{\mathrm{T}}\mathbf{YU}^{-1} = \mathbf{P}_{u2}^{\mathrm{T}}\mathbf{H} \tag{10}$$

After rearranging, (10) can be solved for $\mathbf{\Gamma}$ and $\mathbf{D}$ using the least squares, see (6). In this way the system parameters in the form of state-space matrices of the model (1) are identified using the subspace-based identification method.

4.2 Identified state-space model

System identification was performed on the MATLAB platform using the subspace identification method *n4sid* [4, 5, 34, 35]. For the system identification an arbitrary number of inputs and outputs can be organized in time series of the input–output measurement data. As the output of the algorithm the system matrices of the state-space model (1) are obtained.

Band-limited white noise excitation signals were applied to the four piezoelectric patches as input data and the velocity of the bending vibration was measured as output data for the identification of a state-space model applying the *n4sid* algorithm. The measurement was carried out for 10 s in discrete time using the sampling period T_s=0.001 s. In order to estimate an accurate system order, the identification procedure was repeated several times with different model orders. Finally, an adequate model with the system order n=12 was obtained. The identified model accurately captures the dynamics of the structure within the frequency range of 1 Hz to 500 Hz. Further increase of the system order would not significantly contribute to the improvement of the frequency response in the considered frequency range. On the other hand the computational effort for the controller design would become higher for the increased system order. Furthermore, the identified model of the order 12 fulfills the controllability and observability conditions [36]. The frequency response functions obtained from the identified model for the respective sensor/actuator pairs are represented in Fig. 4. The resonant frequencies at f_1= 13.4 Hz (84.2 rad/s), f_2=72.5 Hz (455.5 rad/s), f_3=198 Hz (1244 rad/s) and f_4=392 Hz (2463 rad/s) correspond to the bending eigenmodes represented in Fig. 3.

5 Model-based controller design

For the purpose of reducing the vibrations of smart beams, caused by a mechanical disturbance, a negative feedback control loop can be established, where the state variables in the state space representation of the structural model are amplified and fed back to the actuators. Thus, assuming a negative feedback control law proportional to the state variables of the system, the control voltage can be written as:

$$\mathbf{u}[k] = -\mathbf{L}\mathbf{x}[k], \tag{11}$$

where $\mathbf{L}$ represents the feedback gain matrix defined according to the control law of interest and $\mathbf{x}$ is the state vector of the design model. Substituting (11) into the state equation of the state space representation, the closed-loop system state equation can be written as

$$\mathbf{x}[k+1] = (\mathbf{\Phi} - \mathbf{\Gamma}\mathbf{L})\mathbf{x}[k]. \tag{12}$$

The feedback gain matrix $\mathbf{L}$ controls the system response through the modification of the closed-loop system poles. Therefore, it is important to find an adequate gain in order to achieve a better damping and quick response of the closed-loop system.

5.1 Optimal control

For the vibration control of smart structures the value of the feedback gain matrix $\mathbf{L}$, described in previous section, is calculated using the optimal control algorithm based on the optimal LQ regulator design. The basic idea of the optimal LQ controller design relies on the feedback gain control law as given in (11), assuming that all the states of the system are completely controllable. The controller design task is to determine the control law in such a way that the performance index

$$J = \sum_{k=0}^{\infty} \left(\mathbf{x}[k]^{\mathrm{T}} \mathbf{Q} \mathbf{x}[k] + \mathbf{u}[k]^{\mathrm{T}} \mathbf{R} \mathbf{u}[k] \right) \tag{13}$$

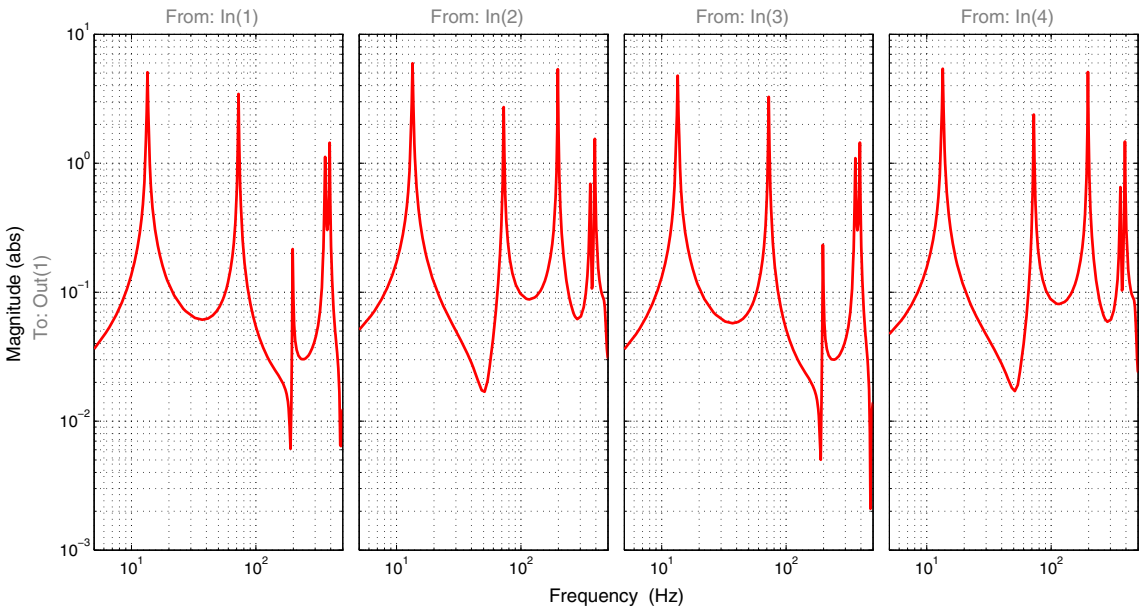

Fig. 4 Frequency response diagrams for the actuator/sensor pairs obtained from the identified state space model

is minimized. The matrices **Q** and **R** in (13) are the designer specified symmetric positive definite weighting matrices. The feedback gain matrix **L** of the optimal LQ control law for a discrete-time state space system is determined through the algorithm for the synthesis of a linear quadratic (LQ) state-feedback regulator by determining:

$$\mathbf{L} = \left(\mathbf{R} + \mathbf{\Gamma}^{\mathrm{T}}\mathbf{P}\mathbf{\Gamma}\right)^{-1}\mathbf{\Gamma}^{\mathrm{T}}\mathbf{P}\mathbf{\Phi}, \tag{14}$$

where **P** is obtained as a solution of the discrete-time Riccati equation in the form [37]:

$$\mathbf{\Phi}^{T}\mathbf{P}\mathbf{\Phi} - \mathbf{P} - \mathbf{\Phi}^{T}\mathbf{P}\mathbf{\Gamma}\left(\mathbf{R} + \mathbf{\Gamma}^{T}\mathbf{P}\mathbf{\Gamma}\right)^{-1}\mathbf{\Gamma}^{T}\mathbf{P}\mathbf{\Phi} + \mathbf{Q} = \mathbf{0} \tag{15}$$

which can be, after rearrangement, written in the form [4]:

$$\mathbf{P} = \mathbf{Q} + \mathbf{\Phi}^{\mathrm{T}}\mathbf{P}\mathbf{\Phi} - \mathbf{\Phi}^{\mathrm{T}}\mathbf{P}\mathbf{\Gamma}\left(\mathbf{R} + \mathbf{\Gamma}^{\mathrm{T}}\mathbf{P}\mathbf{\Gamma}\right)^{-1}\mathbf{\Gamma}^{\mathrm{T}}\mathbf{P}\mathbf{\Phi}. \tag{16}$$

The choice of the weighting matrices **Q** and **R** in the performance index is designer dependant and it is based on the relative importance of the various states and controls. The trade-off between the control effort and the system response determines the choice of the weighting matrices. In general, the weighting matrices are chosen in such a way that large input signals are penalized by increasing the value of the matrix **R** and faster response of appropriate state variables is achieved by increasing the values of appropriate elements in the weighting matrix **Q**.

5.2 State estimation using Kalman filter

Since the state variables of the state space model obtained through the system identification procedure do not represent variables which can be directly measured und thus cannot be used directly in the feedback gain control law (11), their estimation is necessary using an observer. Observer design which is based on the observer pole assignment, like in the case of the Luenberger observer [38], is strongly dependent on the choice of the observer poles and their relation to the plant and closed-loop poles. Such observer design would in turn require appropriate observer pole shifting with regard to the closed-loop poles, since the observer poles must be "faster" then the plant, i.e. closed-loop poles, which means, they should be pulled further left from the imaginary axis in the s-plane, by the continuous-time controller design. The controller considered in this paper is a discrete-time controller, designed for a discrete-time plant model obtained through the subspace identification procedure. Therefore the pole shifting is not a very convenient technique for the observer design when applied to discrete-time models. A comprehensive methodology requires thinking in terms of both the continuous-time and mapped discrete-time z-plane pole locations. Furthermore, the pole assignment technique is not convenient for the multiple-input multiple-output (MIMO) systems, since it does not provide a unique solution. Optimal LQ controller on the other hand provides an optimal solution in the sense of minimizing the performance index (13), by finding an appropriate trade-off between penalizing large control inputs and speeding up the state variables' convergence towards the zero steady-state value, penalizing in this way large state estimation errors in the state transient responses. Pole placement procedure would not give satisfactory result in this case, actually it would require too much trial-and-error effort to find an appropriate pole combination which would result in a satisfactory closed-loop response. This is the reason why the linear quadratic controller represents the authors' favorable feedback design method in this case.

On the other hand, the stability of the closed-loop system with an observer designed based on the pole placement procedure is very sensitive to the choice of the observer poles. In the presence of the process and/or measurement noise, the observer designed for ideal case without noise may introduce instability of the closed-loop. The Kalman filter as observer in the feedback closed-loop system overcomes this drawback. It can successfully meat the requirements of the state estimation in the presence of the white-noise type random measurement or process noise [4]. Therefore the states of the identified model are estimated here by the Kalman estimator, which plays the observer role in the closed loop-system. For a continuous time system, the Kalman estimator equations have in principle the same form as the full-order observer equations, the difference is in the assessment of the observer gain matrix. In the case of Kalman estimator, the estimator gain matrix must take into account for the presence of measurement and/or process noise and it is designed in such a way to minimize the observer estimation error. For the practical implementation within a hardware-in-the-loop system with dSPACE, considered in this paper in combination with discrete-time identified state space model, a discrete-time Kalman estimator is designed.

In a general form of the state space model, the state and output equations are influenced by the process and measurement noise. A general discrete-time state space model, which includes the process noise $\boldsymbol{w}[k]$ and the measurement noise $\boldsymbol{v}[k]$, is assumed in the form (1).

Process and measurement noise represent white noise, i.e. they are random sequences with zero mean:

$$E\{\,\boldsymbol{w}[k]\,\} = E\{\,\boldsymbol{v}[k]\,\} = 0 \tag{17}$$

and they have no time correlation:

$$E\,\boldsymbol{w}(i)\boldsymbol{w}^{\mathrm{T}}(j) = E\boldsymbol{v}(i)\boldsymbol{v}^{\mathrm{T}}(j) = 0 \;\text{ if }\; i \neq j. \tag{18}$$

Covariances or mean square noise levels are defined as:

$$E\left\{\,\boldsymbol{w}[k]\boldsymbol{w}^{\mathrm{T}}[k]\,\right\} = \mathbf{R}_{w}, \quad E\left\{\,\boldsymbol{v}[k]\boldsymbol{v}^{\mathrm{T}}[k]\,\right\} = \mathbf{R}_{v} \tag{19}$$

The underlying idea of the estimator design is to construct an appropriate model of the plant dynamics, such that the state variables of the model can represent the estimates of the real state variables. This underlying idea is extended in the case of a prediction estimator by introducing the feedback system with the estimated output error as the feedback, where measurements at the time k are used for obtaining an estimate of the state vector at the time $k+1$. Design of the Kalman estimator is performed according to the algorithm supported by the Matlab/Control System Toolbox. The algorithm is explained in more detail in [4, 33]. A summary of the Kalman estimator equations is formulated as:

$$\hat{\mathbf{x}}[k+1\,|\,k] = \mathbf{\Phi}\hat{\mathbf{x}}[k\,|\,k-1] + \mathbf{\Gamma}\mathbf{u}[k] + \mathbf{K}(\,\mathbf{y}[k] - \mathbf{C}\hat{\mathbf{x}}[k\,|\,k-1] - \mathbf{D}\mathbf{u}[k]\,) \tag{20}$$

$$\begin{bmatrix}\hat{\mathbf{y}}[k\,|\,k]\\ \hat{\mathbf{x}}[k\,|\,k]\end{bmatrix} = \begin{bmatrix}\mathbf{C}(\mathbf{I}-\mathbf{MC})\\ \mathbf{I}-\mathbf{MC}\end{bmatrix}\hat{\mathbf{x}}[k\,|\,k-1] + \begin{bmatrix}(\mathbf{I}-\mathbf{CM})\mathbf{D} & \mathbf{CM}\\ -\mathbf{MD} & \mathbf{C}\end{bmatrix}\begin{bmatrix}\mathbf{u}[k]\\ \mathbf{y}[k]\end{bmatrix} \tag{21}$$

where: $\hat{\mathbf{x}}[k\,|\,k+1]$ represents the estimate of $\mathbf{x}[k+1]$ given the measurements $\mathbf{y}[k]$, $\mathbf{y}[k-1]$, ... $\hat{\mathbf{x}}[k\,|\,k]$ is the estimate of $\mathbf{x}[k]$ given the measurements: $\mathbf{y}[k]$, $\mathbf{y}[k-1]$, ... and $\hat{\mathbf{y}}[k\,|\,k]$ are corresponding output estimates.

The gain matrices $\mathbf{K}$ and $\mathbf{M}$ are derived by solving corresponding discrete Riccati equation. The innovation gain $\mathbf{M}$ is used to update the prediction $\hat{\mathbf{x}}[k\,|\,k-1]$ using the new measurement $\mathbf{y}[k]$. $\mathbf{K}$ represents the feedback gain matrix of the prediction estimator.

The Kalman estimator design problem is treated as a weighted recursive least squares estimation problem. The feedback gain matrix $\mathbf{K}$ is based on minimizing the estimation error $\mathbf{e}[k] = \mathbf{x}[k] - \hat{\mathbf{x}}[k]$. The equations for computing the feedback gain $\mathbf{K}$ have a striking resemblance to the equations for computing the optimal LQ gain. The Kalman filter implementation requires a priori knowledge of the process noise magnitude $\mathbf{R}_w$ and the measurement noise magnitude $\mathbf{R}_v$. The value for $\mathbf{R}_v$ in a given actual design problem can be chosen based on the sensor accuracy. Here it should also be noted that the assumption about the process noise being the white noise is introduced in order to simplify solving of the optimization problem. Physically $\mathbf{R}_v$ is often associated with unknown disturbances. In the case when a random disturbance is a colored noise (time correlated), it can be accurately modeled by the augmenting $\mathbf{\Phi}$ with a coloring filter which converts a white noise input into a time correlated noise. Due to the complexity it is not done in practice. Rather, the disturbances are assumed to be white and the noise intensity is adjusted to give acceptable results in the presence of expected disturbances.

In the investigated problem, the state estimator was implemented in the feedback closed-loop control system with the estimator gain $\mathbf{K}$ calculated based on the Kalman filter and the feedback gain matrix $\mathbf{L}$ calculated for the optimal LQ controller. Block diagram of the control system is represented in Fig. 5.

Based on the separation principle of the controller/observer design, the feedback gain $\mathbf{K}$ for the state estimation was determined using the Kalman filter algorithm, and implemented for the state estimation within the closed-loop system in Fig. 5. Estimated states, which cannot be measured directly, are multiplied by the feedback gain $\mathbf{L}$ and fed back to the system input, as the control input $\mathbf{u}$. Together with the output measurements $\mathbf{y}$, control input $\mathbf{u}$ represents at the same time the input to the state estimator. The advantage of the Kalman estimator implemented here, over the full order state observer can be seen in the fact, that the state estimation is possible despite the process or the measurement noise. Assumption that the process and/or the measurement noise can be modeled as the white noise, where only the process and the measurement noise covariances are required as the noise parameters for the input to the estimator algorithm design, makes the Kalman estimator a suitable solution to a wide range of practical estimation problems, where implementing merely the full-order observer would not give satisfactory results in the presence of the measurement and/or the process noise.

It is necessary to emphasize at this point, that the concept of the Kalman estimator relies on the state estimation where only control inputs $\mathbf{u}$ and the output measurements $\mathbf{y}$ together with the given noise covariances $\mathbf{R}_w$ and $\mathbf{R}_v$ are required for the estimation of the states in the presence of process/plant and/or measurement noise. Excitations assumed to be the white noise cover a wide range of excitations which can

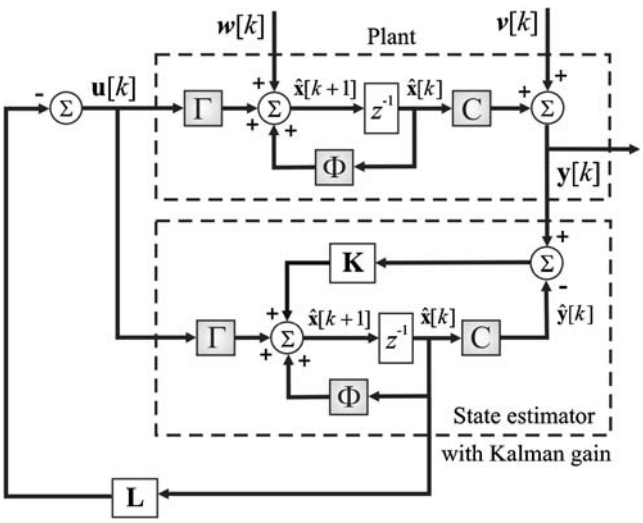

Fig. 5 Block diagram of the feedback control system with state estimator

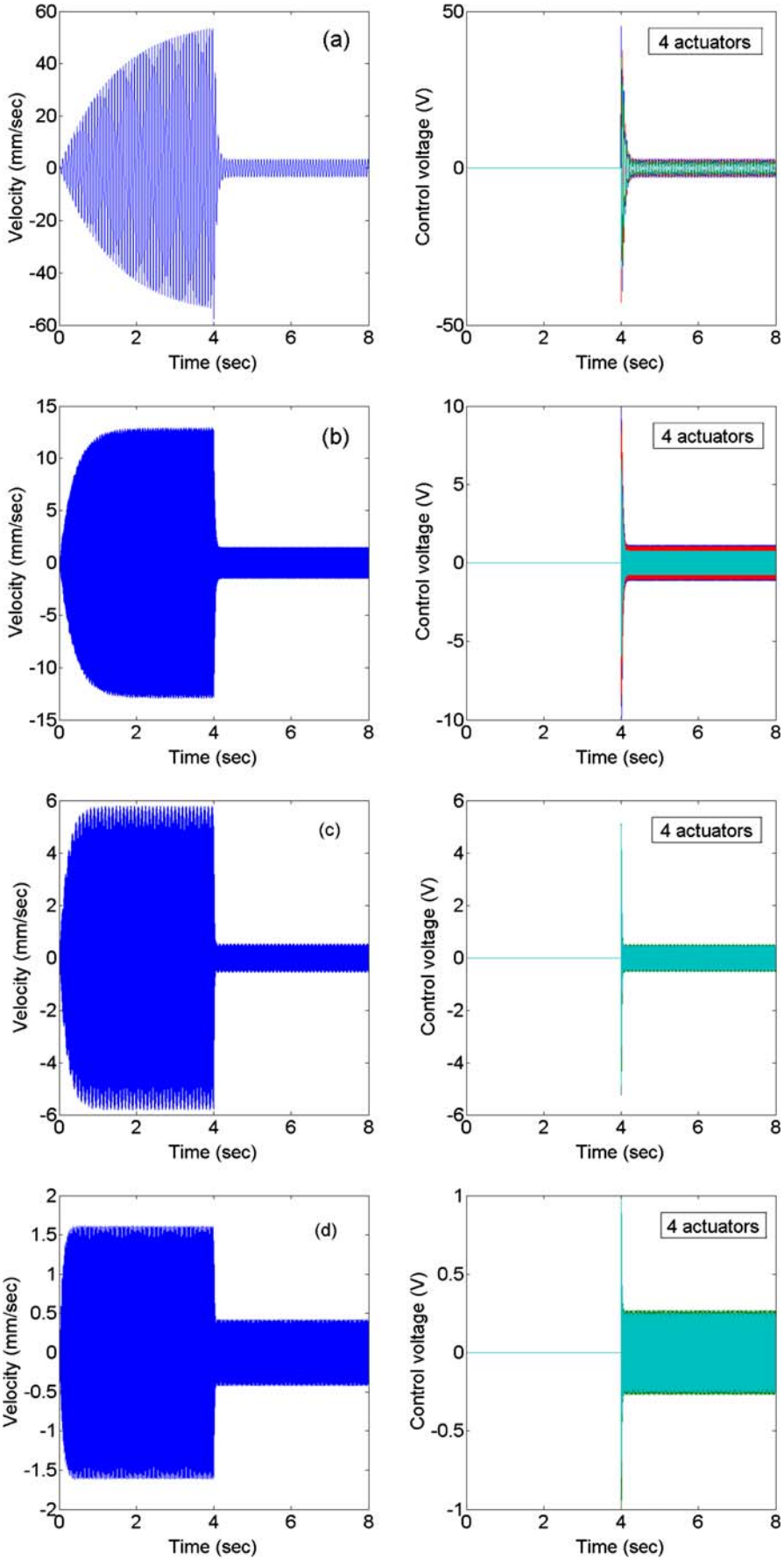

Fig. 6 Simulated sensor signal (velocity) and control voltage signals of uncontrolled and controlled (after 4 s) system, due to a harmonic excitation force: $F(t) = A\sin(2\pi \cdot f_i t)$; **(a)** f_1=13.4 Hz, **(b)** f_2=72.5 Hz, **(c)** f_3=198 Hz, **(d)** f_4=392 Hz

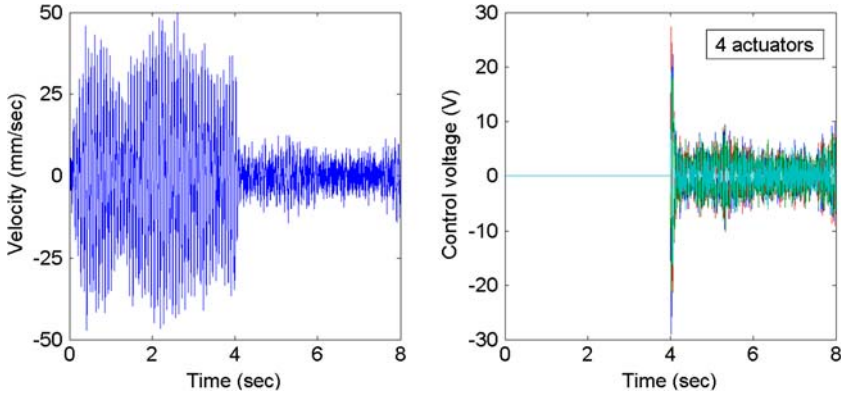

Fig. 7 Simulated sensor signal (velocity) and control voltage signals of uncontrolled and controlled (after 4 s) system, due to a white noise force disturbance

be met in many practical problems. As such they are not considered as elements of the known inputs to the plant or estimator in the case of the Kalman estimator design (as it would be the case with the full-order observer, which should be designed to operate in the presence of disturbances). In the Kalman estimator design procedure, the information about the process/measurement noise is required only in terms of the given parameters $\mathbf{R}_w$ and $\mathbf{R}_v$, the covariances of the process and the measurement noise, respectively. This is what makes the Kalman estimator so powerful and superior over the full-order state observer for the much realistic implementation cases in the presence of noise.

6 Investigation results

The objective of this paper is to show the complete procedure of the smart structures control using selected methods for the model development and controller design presented in the previous sections. The aim of the implementation is the control of a smart piezoelectric structure in the sense of vibration suppression, as described in section 2. Through the experimental application of control and simulation results, the possibilities of the successful vibration control are shown.

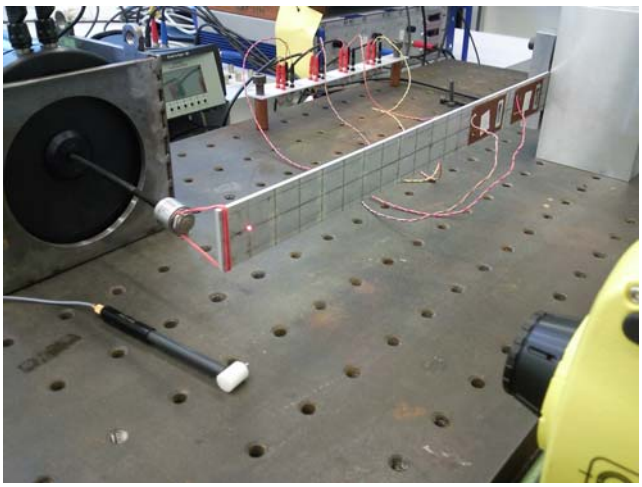

Fig. 8 Experimental rig for validation of the control system based on the identified model

6.1 Closed loop simulation

For the solution of the control task an optimal LQ controller in combination with a Kalman filter is designed (based on the procedure in Section 4) in such a way that the vibration amplitudes due to periodic excitation forces with frequencies corresponding to the eigenfrequencies of the clamped beam, are significantly suppressed in comparison with the uncontrolled case. Simulation results of the controller design, with periodical and random excitation forces are represented in Figs. 6 and 7.

Simulated exciting forces $F(t) = A\sin(2\pi \cdot f_i t)$ exerted to the free end of the beam were chosen with regard to the resonant bending eigenfrequencies f_i of the beam. The optimal LQ control system was designed with the weighting matrices $\mathbf{Q} = \mathbf{C}^{\mathrm{T}}\mathbf{C}$ and $\mathbf{R} = 0.1 \times \mathbf{I}_{4\times 4}$. For the Kalman filter design, it is assumed in the state estimation procedure that only the sensor voltage (vibration velocity) is measured. Furthermore, a plant noise vector (force disturbance) with $\mathbf{R}_w = 100 \times \mathbf{I}_{4\times 4}$ and a sensor noise disturbance with $\mathbf{R}_v = 10$ are considered for the definition of the noise correlation matrices and Kalman feedback gain design.

Diagram 6(a) – (d) represents the uncontrolled and controlled (after 4 s) vibration velocity of the beam, due to harmonic excitation forces with frequencies corresponding to the 1st, 2nd, 3rd and 4th bending eigenfrequency of the clamped beam respectively, as well as the corresponding control signals (actuating voltages on piezo patches). The uncontrolled and controlled (after 4 s) vibration velocity of the beam due to a white noise force disturbance and the corresponding actuating voltages on piezo actuator patches are represented in Fig. 7. In both cases, periodical and random excitation, a significant reduction of the vibration magnitudes can be observed in the presence of the controller.

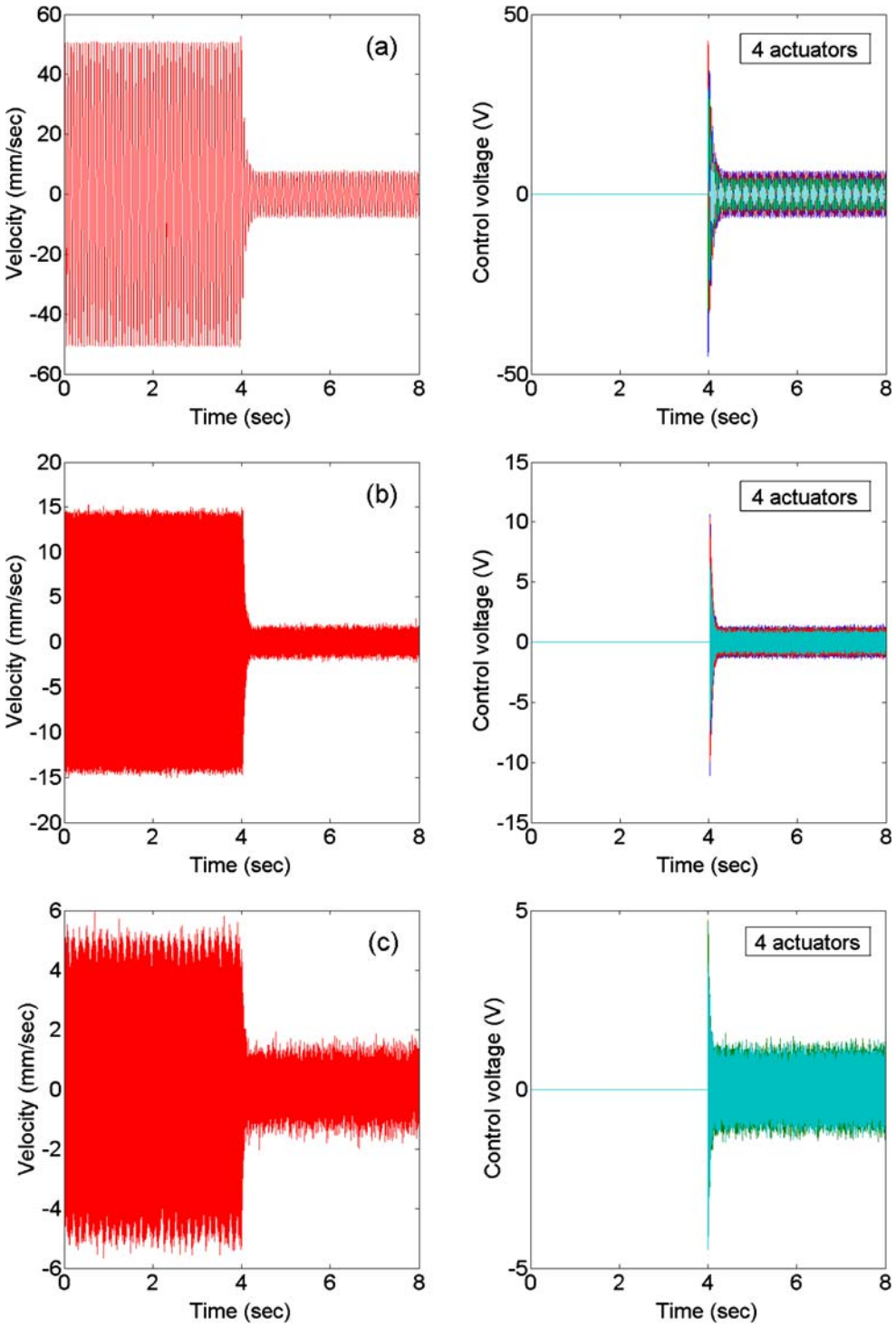

Fig. 9 Experimentally determined sensor signal (velocity) and control voltage signals of uncontrolled and controlled (after 4 s) system, due to a harmonic excitation force: $F(t) = A\sin(2\pi \cdot f_i t)$; **(a)** f_1=14.5 Hz, **(b)** f_2=72.6 Hz, **(c)** f_3=202 Hz

6.2 Experimental implementation

For the purpose of experimental validation, the identified model coupled with the Kalman state estimator and optimal LQ controller designed based on the identified model are implemented within a real time configuration. The closed loop system for the active vibration control of the beam is implemented on the real time data acquisition platform of the dSPACE system with sampling frequency of 1 kHz. The task of the control is to suppress the vibration magnitudes of the sensor signal in time domain an accordingly to reduce the resonance peaks in the frequency domain. Therefore, investigations are carried out both in the time domain and in the frequency domain by means of the experimental rig represented in Fig. 8.

For the analysis in the time domain the shaker, represented in Fig. 8, is used. The shaker is connected to the tip of beam with a rubber band, in order to excite the beam with periodic forces. The sinusoidal excitation signal for the shaker is generated in Simulink and lead out through the dSPACE DAC board. The frequency of the sine signal corresponds to the eigenfrequencies to be controlled. The excitation frequencies for the experimental investigation were fine adjusted experimentally to the values which cause greatest vibration magnitudes, so that disturbances correspond to the system's actual resonant states. The response of the sensor for the uncontrolled and controlled system (after 4 s) and the corresponding control signals in the time domain are represented in Fig. 9. Diagrams shown on the left hand side represent the velocity magnitudes of the beam measured by dSPACE ADC board and diagrams shown on the right hand side represent the voltages at the piezo actuator patches generated by dSPACE DAC board. These results were obtained using the hardware-in-the-loop system with the dSPACE Real-Time Interface platform. The experimental results show, that the application of the control results in an obvious reduction of the vibration amplitudes.

Successful performance of the controlled system is demonstrated for the case of the initial displacement disturbance type as well. Free vibrations of the beam caused by an initial displacement applied to the tip of the beam are comparable with impulse disturbance vibrations. The free vibration response (velocity) of the open-loop and closed-loop system subjected to an initial displacement of 8 mm is measured using the laser vibrometer at the point, which is located 22 mm away from the free end, and it is represented in Fig. 10. Designed controller attenuates significantly the magnitudes of the free end displacement. The closed-loop 5 % settling time is equal to 0.3 s, which reveals a great improvement of the response attenuation when compared with the open-loop one (7.9 s).

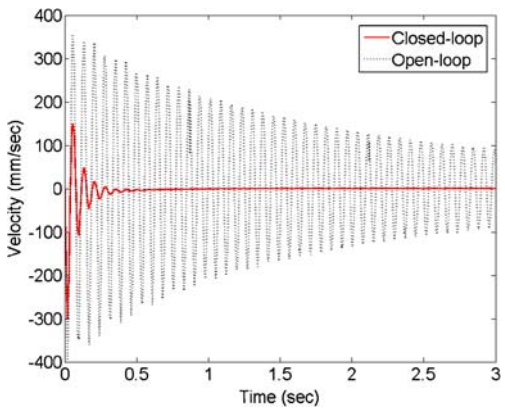

Fig. 10 Free vibration response (velocity) of the controlled and uncontrolled system

The effect of the control is also documented in the frequency domain by obtaining frequency response functions from measured input and output signals. The frequency response functions between the sensor signal (laser vibrometer) as the output and the impulse excitation by an impact hammer as an input were determined using the experimental rig represented in Fig. 8, in this case with the hammer instead of shaker. The free end of the beam was excited using the impact hammer and the response from the sensor was measured, for both controlled and uncontrolled case. Controlled and uncontrolled frequency response functions are represented in Fig. 11 for the frequency range of up to 500 Hz. The figure shows significant vibration suppression in terms of the peak amplitudes reduction for the controlled eigenfrequencies. Especially in the lower frequency range, the designed controller significantly reduces the peak magnitude at the first resonant frequency for approximately 32 dB.

7 Conclusion

This paper presents a design approach for actively controlled smart structures, with the focus on structural control with piezoelectric materials as active elements. In the overall design approach several phases are considered, such as modeling, controller design, simulation and experimental implementation. The main control objective is the active vibration suppression of a smart structure, cantilever aluminum beam, controlled by four piezoelectric ceramic patches. For the active vibration control of the structure, the bending vibration velocity is measured by a laser Doppler vibrometer, which provides the feedback signal in the active control algorithm.

A subspace-based identification procedure is used to obtain a state-space model of the system from its input–output measurement data. Through the comparison of measured and model-based assessed eigenfrequencies, a good

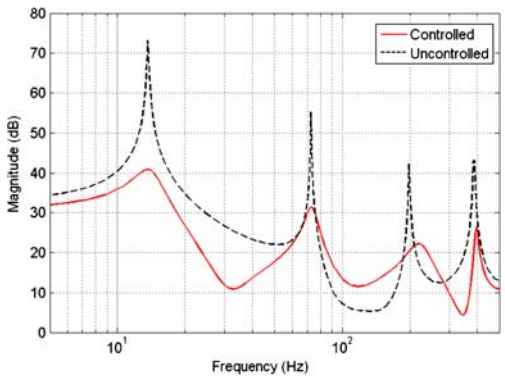

Fig. 11 Frequency response of the controlled and uncontrolled system

representation of the structural dynamics by the identified model was demonstrated and it was shown to be a valuable tool for the controller design. In this study, an optimal LQ feedback strategy is used for the controller design, which provides the designer with lots of flexibility to perform trade-offs among various performance criteria. The optimal LQ controller requires a full knowledge of the state variables, in order to generate the control input. Therefore, a Kalman filter is used as an observer, in order to estimate the unmeasurable state variables.

Control problems treated in this work assume a specific class of excitations, which from the vibration point of view can be regarded as a worst study case due to the possibility of resonance. Those are periodic sinusoidal excitations with frequencies corresponding to the eigenfrequencies in the frequency range of interest. The suppression of vibrations caused by such excitations and disturbances represents therefore an important task which is, in this case, demonstrated to be successfully accomplished by applying the control system to the considered piezoelectric smart structure. However, in some cases observation and control spill-over problems related with unobserved model dynamics may compromise stability, if the unmodeled modes are excited by the controller.

Acknowledgment The authors gratefully acknowledge the funding by the German Research Foundation (DFG) within Collaborative Research Center under grant SFB-837/A2.

References

1. S. Herold, Simulation des dynamischen und akustischen Verhaltens aktiver Systeme im Zeitbereich, Ph.D. thesis. (TU Darmstadt, Germany, 2003), http://tubiblio.ulb.tu-darmstadt.de/37184/, Accessed 26 April 2012
2. A. Benjeddou, Advances in piezoelectric finite element modeling of adaptive structural elements: a survey. Comput. Struct. **76**, 347–363 (2000)
3. I. Chopra, Review of state of art of smart structures and integrated systems. AIAA J. **40**, 2145–2187 (2002)
4. T. Nestorović, Controller Design for the Vibration Suppression of Smart Structures. (Fortschritt-Berichte VDI, Vol. 8, Düsseldorf, Germany, 2005) ISBN 3-18-507108-5
5. T. Nestorović, U. Gabbert, Subspace-based frequency analysis of a smart acoustic structure, Facta Universitatis Series Mechanics Automatic Control and Robotics. 7, 209–220 (2008)
6. T. Nestorović Trajkov, H. Köppe, U. Gabbert, Direct model reference adaptive control (MRAC) design and simulation for the vibration suppression of piezoelectric smart structures. Commun. Nonlinear Sci. Numer. Simul. **13**, 1896–1909 (2008). doi:10.1016/j.cnsns.2007.03.025
7. T. Nestorović Trajkov, U. Gabbert, Active control of a piezoelectric funnel-shaped structure based on subspace identification. Struct. Contr. Health Monit. **13**, 1068–1079 (2006). doi:10.1002/stc.94
8. T. Nestorović Trajkov, H. Köppe, U. Gabbert, Active Vibration Control Using Optimal LQ Tracking System with Additional Dynamics. Int. J. Control. **78**, 1182–1197 (2005). doi:10.1080/00207170500163383
9. C.M.A. Vasques, J. Dias Rodrigues, Active vibration control of smart piezoelectric beams: Comparison of classical and optimal feedback control strategies. Comput. Struct. **84**, 1402–1414 (2006)
10. E. Grasso, D. Pesotski, H. Janocha, Self-sensing piezoelectric actuators for vibration control purposes, Actuator, Proc. 12th International Conference on New Actuators. (Bremen, 2010), pp. 151–154
11. A. Azizi, L. Dourali, S. Zareie, F.P. Rad, Control of Vibration Suppression of an Smart Beam by Pizoelectric Elements, Second International Conference on Environmental and Computer Science ICECS '09. (2009), pp. 165–169
12. A. Maccari, Vibration Control for the Primary Resonance of a Cantilever Beam by a Time Delay State Feedback. J. Sound Vibrat. **259(2), 241–251 (2003)**
13. O.F. Kircali, Y. Yaman, V. Nalbantoglu, M. Sahin, F.M. Karadal, F.D. Ulker, Spatial control of a smart beam. J. Electroceram. **20**(3–4), 175–185 (2008)
14. Jac-Eung Oh, Soo-Hong Park, Jin-Seok Hong und Jun Shin, Active vibration control of flexible cantilever beam using piezo actuator and Filtered-X LMS algorithm. KSME International Journal continued by J. Mech. Sci. Technol. 12 (4), 665–671 (1998), www.springerlink.com/content/y86431n314mn7884/. Accessed 27. April 2012
15. H. Tjahyadi, F. He, K. Sammut, Multi-mode vibration control of a flexible cantilever beam using adaptive resonant control. Smart Mater. Struct. **15**, 270–278 (2006)
16. J. Fei, Active vibration control of flexible steel cantilever beam using piezoelectric actuators, Proceedings of the Thirty-Seventh Southeastern Symposium on System Theory SSST '05. (2005), pp. 35–39
17. R. Heuer, Vibration Control of Linear Elastic Beam Structures with Spatial Local Nonlinearities, in Advanced Dynamics and Model-Based Control of Structures and Machines, ed. H. Irschik, M. Krommer and A.K. Belyaev (Springer-Verlag, Wien, 2012), p. 101–108, doi:10.1007/978-3-7091-0797-3_12
18. A. Joshi, Theoretical and Experimental Studies on Vibration Control in Cantilever Beams Using DC Magnets. J. Vib. Control. **10**, 995–1008 (2004)
19. T.C. Manjunath, B. Bandyopadhyay, Vibration Control of a Smart Structure Using periodic Output Feedback Technique. Asian J. Control. **6**(1), 74–87 (2004)
20. L. Li, G. Song, J. Ou, Adaptive fuzzy sliding mode based active vibration control of a smart beam with mass uncertainty. Struct. Control Health Monit. **18**, 40–52 (2011). doi:10.1002/stc.356
21. F. Wang, G.J. Tang, D.K. Li, Accurate modeling of a piezoelectric composite beam. Smart Mater. Struct. **16**(5), 1595–1602 (2007)
22. C.M.A. Vasques, J. Dias Rodrigues, Active vibration control of a smart beam through piezoelectric actuation and laser vibrometer sensing: simulation, design and experimental implementation. Smart Mater. Struct. **16**(2), 305–316 (2007)
23. J. Lin, Y.B. Zheng, Vibration suppression control of smart piezoelectric rotating truss structure by parallel neuro-fuzzy control with genetic algorithm tuning, J. Sound Vibrat. (2012) doi: 10.1016/j.jsv.2012.04.001
24. M.S. Rechdaoui, L. Azrar, Active control of secondary resonances piezoelectric sandwich beams. Appl. Math. Comput. **216**(11), 3283–3302 (2010). doi:10.1016/j.amc.2010.04.055
25. T. Nestorović, D. Marinković, G. Chandrashekar, Z. Marinković, M. Trajkov, Implementation of a user defined piezoelectric shell element for analysis of active structures. Finite Elem. Anal. Des. **52**, 11–22 (2012). doi:10.1016/j.finel.2011.11.006
26. Y.A. Zhuk, I.A. Guza, C.M. Sands, Monoharmonic approximation in the vibration analysis of a sandwich beam containing piezoelectric layers under mechanical or electrical loading. J. Sound Vibrat. **330**(17), 4211–4232 (2011). doi:10.1016/j.jsv.2011.04.012

27. K. Yamadaa, H. Matsuhisa, H. Utsuno, A new method for accurately determining the modal equivalent stiffness ratio of bonded piezoelectric structures. J. Sound Vibrat. **331**(14), 3317–3344 (2012). doi:10.1016/j.jsv.2012.02.028
28. J. Warminski, M. Bochenski, W. Jarzyna, P. Filipek, M. Augustyniak, Active suppression of nonlinear composite beam vibrations by selected control algorithms. Commun. Nonlinear Sci. Numer. Simul. **16**(5), 2237–2248 (2011). doi:10.1016/j.cnsns.2010.04.055
29. H.A. El-Gohary, W.A.A. El-Ganaini, Vibration suppression of a dynamical system to multi-parametric excitations via time-delay absorber. Appl. Math. Model. **36**(1), 35–45 (2012). doi:10.1016/j.apm.2011.05.034
30. S.X. Xu, T.S. Koko, Finite element analysis and design of actively controlled piezoelectric smart structures. Finite Elem. Anal. Des. **40**, 241–262 (2004)
31. P. Van Overschee, B. De Moor, Subspace Identification for Linear systems: Theory, Implementation, Applications. (Kluwer Academic Publishers, 1996) Vol. 1
32. M. Viberg, Subspace-based state-space identification. Circ. Syst. Signal Process. **21**, 23–37 (2002). doi:10.1007/BF01211649
33. G.F. Franklin, J.D. Powell, M.L. Workman, Digital Control of Dynamic Systems, 3rd edition. (Addison-Wesley Longman, Inc. 1998)
34. P. Van Overschee, B. De Moor, N4SID: Subspace algorithms for the identification of combined deterministic-stochastic systems. Automatica **30**, 75–93 (1994)
35. L. Ljung, System Identification Toolbox™ 7: User's Guide, Natick, MA, USA. (The Mathworks Inc. 2010)
36. R.J. Vaccaro, Digital Control: A State-Space Approach. (McGraw-Hill, Inc. 1995)
37. Mathworks, Matlab R2012a Documentation - Control System Toolbox, www.mathworks.de/help/toolbox/control/, Accessed 27 April 2012
38. D.G. Luenberger, An Introduction to Observers. IEEE Trans. Autom. Control. **AC-16**(6), 596–602 (1971). doi:10.1109/TAC.1971.1099826